A Total Variation Based Reconstruction Algorithm for 3D Ultrasound

Manya V. Afonso* and João M.R. Sanches

Instituto de Sistemas e Robótica, Instituto Superior Técnico, Lisbon, Portugal

Abstract. This paper presents an algorithm for reconstructing a three dimensional image from a set of noisy two dimensional images, corrupted with Rayleigh distributed multiplicative noise, which is the observational model for Ultrasound imaging. The proposed method performs a variable splitting to introduce an auxiliary variable to serve as the argument of the 3D total variation term. Applying the Augmented Lagrangian framework and using an iterative alternating minimization method leads to simpler problems involving TV minimization with a least squares term. The resulting Gauss Seidel scheme is an instance of the Alternating Direction Method of Multipliers (ADMM) method, for which convergence is guaranteed. Experimental results show that the proposed method is faster and achieves a lower mean square error than existing methods.

Keywords: 3D reconstruction, multiplicative noise, ultrasound, convex optimization, total variation.

1 Introduction

Ultrasound (US) has emerged as a popular medical imaging modality in a number of medical imaging applications because of its lower cost, wide reach, flexibility, lack of radiation, and intra-operability [8], [15], [5]. Three dimensional (3D) US imaging is being increasingly used for characterizing diseases such as carotid atherosclerosis, requiring a 3D volume to be reconstructed from a series of 2D slices. The slices can be acquired mechanically in a predetermined manner, or freehand wherein the user can manually position and orient the probe.

Due to the impracticality of slicing over the entire volume, voxel values of the 3D object are available for only a small set of the 3D positions. Hence, the reconstruction algorithm needs to estimate the volume from a set of partial observations. US images are corrupted by multiplicative noise called speckle, for which the Rayleigh distribution has been assumed [13].

Existing interpolation algorithms such as the Pixel Nearest Neighbor (PNN) [11], Voxel Nearest Neighbor (VNN) [11], Pixel-Based Interpolation with Distance Weighting (PBM-DW) [9], etc do not use any regularization or apriori

* This work was supported by *Fundação para a Ciência e Tecnologia* (FCT), Portuguese Ministry of Science and Higher Education, through a Post-doctoral fellowship (contract no. SFRH/BPD/79011/2011) and FCT project (PEst-OE/EEI/LA0009/2011).

J.M. Sanches, L. Micó, and J.S. Cardoso (Eds.): IbPRIA 2013, LNCS 7887, pp. 149–156, 2013.

information about the volume to be reconstructed. A comprehensive review of interpolation methods for US reconstruction can be found in [15]. In [14], a despeckling method was proposed formulating the estimation problem as a convex optimization problem with total variation (TV) regularization, under the assumption that the solution is piece-wise smooth and the speckle noise is Rayleigh distributed. A reconstruction method called 3D Rayleigh Log Total Variation (3D RLTV) was proposed in [13], and consists of a pixel-based maximum likelihood interpolation step, followed by applying the despeckling algorithm from [14]. This formulation was also used in [3], for the context of Synthetic Aperture Radar (SAR) image denoising. The Nakagami distribution was assumed as the statistical model in the denoising method presented in [17]. In [6], a denoising method was presented assuming that the multiplicative noise (in natural images) was one-sided exponentially distributed, and with an ℓ_1 data fidelity term.

In this work, we propose a fast method to solve the denoising and reconstruction problems with multiplicative noise assuming Rayleigh statistics. We extend the convex denoising formulation from [14] and [3] to the more general problem of reconstruction from partial observations, and solve it using the Augmented Lagrangian (AL)/Alternating Direction Method of Multipliers (ADMM) framework [7] which leads to an alternating minimization in which at every iteration a sequence of simpler problems has to be solved. This approach was experimentally found to achieve a good balance between computation time and accuracy.

We will formulate the problem of reconstructing the 3D volume in Section 2. In Section 3 we apply the AL/ADMM framework to our optimization problem to obtain the proposed method. In Section 4, we present some results on 3D despeckling and reconstruction, with synthetic and real US images.

2 Problem Formulation

Representing the 3D volumes in vector format, say, in lexicographic ordering, the observation model with multiplicative speckle noise is

$$\mathbf{y} = (\mathbf{A}\mathbf{x}).\eta, \tag{1}$$

where $\mathbf{x} \in \mathbb{R}^n$ is the volume to be estimated, n is the number of voxels, $\mathbf{y} \in \mathbb{R}^m$ is the vector representation of the set of observed 2D slices, m is the number of observed voxels, $\mathbf{A} \in \{0,1\}^{m \times n}$ is the linear observation operator, and $\eta \in \mathbb{R}^m$ is the speckle field that is multiplied element-wise with the observed volume. The linear operator $\mathbf{A}$ maps a voxel in the 3D space to a pixel in the set of observed slices, and discards the voxels in $\mathbf{x}$ which don't correspond to a pixel in $\mathbf{y}$. Hence, for $m < n$, the matrix $\mathbf{A}$ is essentially the $n \times n$ identity matrix with $n - m$ rows (corresponding to non-observed voxels) removed. The position and orientation of each slice must be known to construct $\mathbf{A}$. For a denoising problem, *i.e.*, when all voxel values are observed, it is equal to the identity matrix $\mathbf{A} = \mathbf{I}$.

For the Radio Frequency envelope images, it is assumed that the observed image follows Rayleigh statistics [12], with the likelihood

$$p(\mathbf{y}|\mathbf{x}) = \prod_{i=1}^{m} \frac{y_i}{(\mathbf{Ax})_\mathbf{i}} \exp\left(-\frac{y_i^2}{2(\mathbf{Ax})_i}\right), \tag{2}$$

where $(\mathbf{Ax})_i$ is the i^{th} element of the sampled vector $\mathbf{Ax}$, and y_i is the i^{th} element of the noisy observed vector $\mathbf{y}$. This leads to the log-likelihood function,

$$E(\mathbf{y}, \mathbf{x}) = -\log\left(p(\mathbf{y}|\mathbf{x})\right) = \sum_{i=1}^{m} \left(\frac{y_i^2}{2(\mathbf{Ax})_i} + \log(\mathbf{Ax})_i\right). \tag{3}$$

To formulate the problem of estimating the volume $\mathbf{x}$, given $\mathbf{y}$ with the statistical model (2), we apply the logarithmic transformation, $\mathbf{f} = \log(\mathbf{Ax})$, and then define the estimation problem as the problem of minimizing the sum of the data fidelity term (3) and a 3D TV regularizer term,

$$\min_{\mathbf{x},\mathbf{f}} \sum_i \left(\frac{y_i^2}{2} e^{-f_i} + f_i\right) + \alpha TV(\mathbf{f}), \qquad \text{subject to} \quad \mathbf{Ax} = e^{\mathbf{f}}, \tag{4}$$

where as before, f_i represents a voxel from the vector representation of $\mathbf{f}$, indexed by the coordinates (i_x, i_y, i_z), $\alpha > 0$ is the regularization parameter, and the regularizer function is the 3D TV function which is given by

$$\begin{aligned} TV(\mathbf{f}) = \sum_i \big((f_{i_x,i_y,i_z} - f_{i_x-1,i_y,i_z})^2 + (f_{i_x,i_y,i_z} - f_{i_x,i_y-1,i_z})^2 + \dots \\ + (f_{i_x,i_y,i_z} - f_{i_x-1,i_y,i_z-1})^2\big)^{\frac{1}{2}} \end{aligned} \tag{5}$$

This formulation is the generalized form of the TV regularized despeckling problem from [14], and can be verified to be convex. For denoising, the problem is,

$$\min_{\mathbf{f}} \sum_i \left(\frac{y_i^2}{2} e^{-f_i} + f_i\right) + \alpha TV(\mathbf{f}). \tag{6}$$

3 Proposed Method

We find the solution of problem (4) by using an approach based on the AL/ADMM framework [7]. In [3], an ADMM based method was presented for solving the denoising problem (6) but without logarithmic compression, for the case of multiple look SAR imaging. We perform a variable splitting in (4) and introduce an auxiliary variable $\mathbf{u}$ to serve as the argument of the TV term, with the constraint $\mathbf{x} = \mathbf{u}$. This leads to the constrained optimization problem,

$$\min_{\mathbf{x},\mathbf{f},\mathbf{u}} \sum_i \left(\frac{y_i^2}{2} e^{-f_i} + f_i\right) + \alpha TV(\mathbf{u}), \qquad \text{subject to} \quad \mathbf{Ax} = e^{\mathbf{u}}, \quad \mathbf{x} = \mathbf{u}. \tag{7}$$

Using the AL, this problem can be shown to be equivalent to,

$$\min_{\mathbf{x},\mathbf{f},\mathbf{u},\mathbf{d_f},\mathbf{d_u}} \sum_i \left(\frac{y_i^2}{2} e^{-f_i} + f_i \right) + \alpha \mathrm{TV}(\mathbf{u}) + \mu_f \|\mathbf{A}\mathbf{x} - e^{\mathbf{f}} - \mathbf{d}_f^k\|_2^2 + \mu_u \|\mathbf{x} - \mathbf{u} - \mathbf{d}_u^k\|_2^2. \tag{8}$$

where $\mu_f, \mu_u > 0$ are the AL penalty parameters, and $\mathbf{d}_f, \mathbf{d}_u$ are the so-called Bregman update vectors [16,10]. The AL algorithm iterates between minimizing the objective function in (8) with respect to $\mathbf{x}$, $\mathbf{f}$ and $\mathbf{u}$, leading to a Gauss-Seidel process (for more details, see [1]) which at iteration k is summarized as,

$$\mathbf{f}^{k+1} = \arg\min_{\mathbf{f}} \sum_i \left(\frac{y_i^2}{2} e^{-f_i} + f_i \right) + \mu_f \|\mathbf{A}\mathbf{x}^{\mathbf{k}} - e^{\mathbf{f^k}} - \mathbf{d}_f^k\|_2^2, \tag{9}$$

$$\mathbf{u}^{k+1} = \arg\min_{\mathbf{u}} \alpha \mathrm{TV}(\mathbf{u}) + \mu_u \|\mathbf{x}^k - \mathbf{u} - \mathbf{d}_u^k\|_2^2, \tag{10}$$

$$\mathbf{x}^{k+1} = \arg\min_{\mathbf{x}} \mu_f \|\mathbf{A}\mathbf{x} - e^{\mathbf{f^{k+1}}} - \mathbf{d}_f^k\|_2^2 + \mu_u \|\mathbf{x} - \mathbf{u}^{k+1} - \mathbf{d}_u^k\|_2^2, \tag{11}$$

$$\mathbf{d}_f^{k+1} = \mathbf{d}_f^k - (\mathbf{A}\mathbf{x}^{\mathbf{k+1}} - e^{\mathbf{f^{k+1}}}), \tag{12}$$

$$\mathbf{d}_u^{k+1} = \mathbf{d}_u^k - (\mathbf{x}^{\mathbf{k+1}} - \mathbf{u}^{k+1}). \tag{13}$$

Problem (10) involves the sum of a quadratic term and a TV term and can be solved using a solver for denoising with additive and Gaussian noise, such as a 3D implementation of Chambolle's algorithm [4]. The objective function in (9) is separable for each voxel f_i, and can be decomposed into m problems,

$$f_i^{k+1} = \arg\min_{f_i} \frac{y_i^2}{2} e^{-f_i} + f_i + \frac{\mu_f}{2} (f_i - u_i^{k+1} - (d_f)_i^k)^2, \tag{14}$$

which can be solved accurately and efficiently using a few iterations of Newton's method [3]. Problem (11) is a least squares minimization,

$$x_i^{k+1} = \arg\min_{x_i} \mu_f \|\mathbf{A}\mathbf{x} - e^{\mathbf{f^{k+1}}} - \mathbf{d}_f^k\|_2^2 + \mu_u \|\mathbf{x} - \mathbf{u}^{k+1} - \mathbf{d}_u^k\|_2^2 \tag{15}$$

$$= \left(\mu_f \mathbf{A}^T\mathbf{A} + \mu_u \mathbf{I}\right)^{-1} \left(\mu_f (e^{\mathbf{f^{k+1}}} + \mathbf{d}_f^k) + \mu_u (\mathbf{u}^{k+1} + \mathbf{d}_u^k) \right) \tag{16}$$

and can be solved efficiently because the structure of $\mathbf{A}$ implies that $(\mu_f \mathbf{A}^T\mathbf{A} + \mu_u \mathbf{I})^{-1}$ is a diagonal matrix. Even though (10) and (9) are not solved exactly, the convergence conditions for ADMM [7] only require that their error sequences decrease monotonically and μ_u and μ_f be positive.

For despeckling, when $m = n$ and $\mathbf{A} = \mathbf{I}$, the procedure is computationally faster because there is one constraint less, and therefore there is no least squares minimization and one less Bregman update in each iteration [2].

4 Experimental Results

We need to evaluate the performance of the proposed method based on two criteria - computational speed and accuracy of reconstruction. To be able to

evaluate the accuracy, we need to have access to a reference noiseless image, or the ground truth. Since in practice, we may not have a ground truth for real data we need to construct a synthetic example to test our proposed method.

We compare our approach against the interpolation based methods - PNN, PBM-DW, and VNN [11],[15], and 3D RLTV [13]. Except for the last, all these methods are non-iterative and do not account for the statistical model.

All experiments were performed on MATLAB on an Ubuntu Linux based laptop, with the Intel i5 processor and 8 GB of RAM. The proposed method was run until the relative difference $\|\hat{\mathbf{x}}^{k+1} - \hat{\mathbf{x}}^k\|_2 / \|\hat{\mathbf{x}}^k\|_2$ fell below 0.01. It was experimentally found that the values for the parameters $\alpha = 100, \mu_u = 50, \mu_f = 50$ worked well in terms of reconstruction error for both synthetic and real US experiments. 3D RLTV was run with the parameters suggested in [13].

4.1 Synthetic Volume

The synthetic experiment uses a volume of size $60 \times 60 \times 60$ and consists of a cylindrical tube with ones in the volume of the cylinder and zeros elsewhere, which is then corrupted with Rayleigh distributed multiplicative noise. With linear mechanical scanning over the z-axis, 30 parallel slices such as one shown in Fig 1(a) are acquired parallel to the xy-plane. Figures 1(b) and 1(c) show the gaps corresponding to missing slices, viewed in the yz- and zx- cross sections, respectively. The corresponding slices of the volume reconstructed using the proposed method are shown in figures 1(d), 1(e), and 1(f). In Fig 3(a) it can be seen that the objective function from (4) plateaus out after some time.

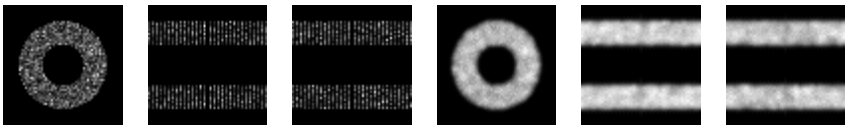

(a) (b) (c) (d) (e) (f)

Fig. 1. Synthetic example (linear mechanical acquisition along z-axis): Cross section of observed volume in (a) xy-, (b) yz- and, (c) zx- planes; CS of reconstructed volume in (e) xy-, (f) yz- and, (g) zx- planes

With freehand acquisition, 30 slices of size 60×60 oriented randomly were acquired, resulting in an observed volume with cross-sectional views as shown in figures 2(a), 2(b) and 2(c). The corresponding slices of the volume reconstructed using the proposed method are shown in figures 2(d), 2(e), and 2(f), and Fig 3(b) shows the evolution of the objective function over time.

The Mean Square Error (MSE) between the original synthetic volume $\mathbf{x}$ and the estimated volume $\hat{\mathbf{x}}$ is computed as, $\text{MSE} = \frac{1}{n}\|\mathbf{x} - \hat{\mathbf{x}}\|_2^2$, where n is the number of voxels. Table 1 compares the proposed method against existing ones in terms of the MSE and computation time, for both linear mechanical and

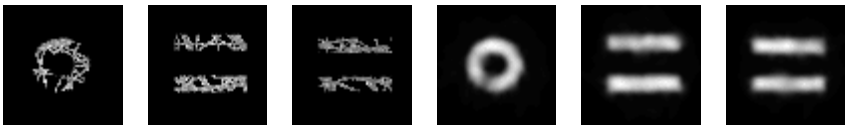

(a) (b) (c) (d) (e) (f)

Fig. 2. Synthetic example (freehand): CS of observed volume in (a) xy-, (b) yz- and, (c) zx- planes; CS of reconstructed volume in (e) xy-, (f) yz- and, (g) zx- planes

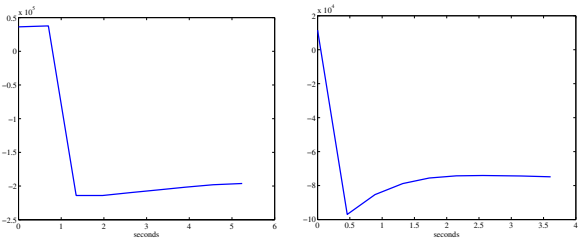

(a) (b)

Fig. 3. Evolution of the objective function for the reconstruction of the synthetic volume, for (a) linear mechanical scanning, (b) freehand acquisition

freehand acquisitions. It can be seen from this table that the proposed method achieves a value of MSE close to the best possible, and only PNN (which is non-iterative) is computationally faster but with a higher MSE. Hence, the proposed method achieves a good balance between computation time and accuracy.

Table 1. Comparison of various reconstruction methods for synthetic data

	Synthetic tube				Carotid US
	Linear mechanical scanning		Freehand scanning		
Algorithm	MSE	Time (sec.)	MSE	Time (sec.)	Time (sec.)
Proposed method	0.039	5.366	0.296	3.806	93.351
PNN	0.103	1.342	0.330	2.012	32.308
PBM-DW	0.101	6.380	0.319	7.348	152.459
VNN	0.166	300.333	0.382	481.216	—
RLTV-3D	0.029	7.410	0.314	7.582	548.671

4.2 Real Ultrasound Data

We then reconstructed a volume from a set of 2D US images of the carotid artery, acquired transversally over a region of length 8 cm. There were 60 slices of size 255×282, each roughly corresponding to an area of 3.9×4 sq.cm. The B-mode images were first stacked together into a volume and then pre-processed to

extract the RF image [12]. Fig 4 shows the cross sectional views of the observed stack of images and the reconstructed volume. The objective function is shown in fig 5(a), and fig 5(b) shows a 3D rendering of the reconstructed volume. The computation times are presented in the last column of table 1. It can be seen that the proposed method is slower than only the non-iterative PNN. Based on the synthetic experiments, we can see that our method achieves a lower MSE than PNN, the only method that is computationally faster.

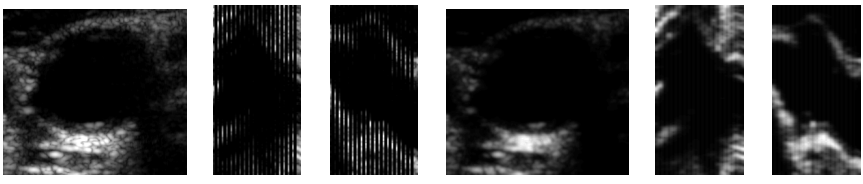

(a) (b) (c) (d) (e) (f)

Fig. 4. Carotid artery: Cross section of observed slices in (a) xy-, (b) yz-, and (c) zx-planes; CS of reconstructed volume in (e) xy-, (f) yz-, and (g) zx- planes

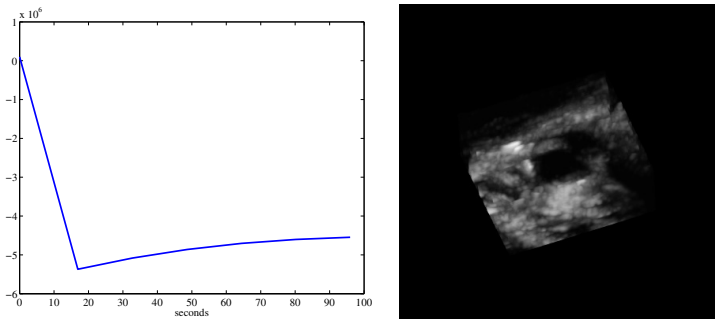

(a) (b)

Fig. 5. Carotid artery: (a) objective function, (b) reconstructed volume

5 Conclusions

We have proposed a fast ADMM-based algorithm for 3D reconstruction with multiplicative speckle noise, assuming Rayleigh statistics. Experiments on synthetic and real US data showed that the proposed method offers a good balance between reconstruction accuracy and computation time. In this work we assumed that the acquired US images of the carotid artery were approximately parallel and evenly spaced. A spatial locator may not always be available. Current and future work includes estimating the slice position by estimating the velocity based on the speckle field after decomposing the reconstructed volume.

References

1. Afonso, M., Bioucas-Dias, J., Figueiredo, M.: An augmented lagrangian based method for the constrained formulation of imaging inverse problems. IEEE Tr. Im. Proc. 20(3), 681–695 (2011)
2. Afonso, M., Sanches, J.: A total variation based denoising algorithm for 3d ultrasound. In: Reconhecimento de Padrões, Portuguese Conference on Pattern Recognition (RecPad 2012), Coimbra, Portugal (2012)
3. Bioucas-Dias, J., Figueiredo, M.: Multiplicative noise removal using variable splitting and constrained optimization. IEEE Transactions on Image Processing 19(7), 1720–1730 (2010)
4. Chambolle, A.: An algorithm for total variation minimization and applications. Journal of Mathematical Imaging and Vision 20(1), 89–97 (2004)
5. Coupé, P., Hellier, P., Azzabou, N., Barillot, C.: 3D freehand ultrasound reconstruction based on probe trajectory. In: Duncan, J.S., Gerig, G. (eds.) MICCAI 2005. LNCS, vol. 3749, pp. 597–604. Springer, Heidelberg (2005)
6. Durand, S., Fadili, J., Nikolova, M.: Multiplicative noise removal using l1 fidelity on frame coefficients. J. Math. Imaging Vis. 36(3) (2010)
7. Eckstein, J., Bertsekas, D.: On the DouglasRachford splitting method and the proximal point algorithm for maximal monotone operators. Mathematical Programming 55(3), 293–318 (1992)
8. Fenster, A., Downey, D.B., Cardinal, H.N.: Three-dimensional ultrasound imaging. Physics in Medicine and Biology 46(5), R67 (2001)
9. Gobbi, D.G., Peters, T.M.: Interactive intra-operative 3D ultrasound reconstruction and visualization. In: Dohi, T., Kikinis, R. (eds.) MICCAI 2002, Part II. LNCS, vol. 2489, pp. 156–163. Springer, Heidelberg (2002)
10. Goldstein, T., Osher, S.: The split Bregman method for ℓ_1 regularized problems. SIAM Journal on Imaging Sciences 2(2), 323–343 (2009)
11. Rohling, R., Gee, A., Berman, L.: A comparison of freehand 3D ultrasound reconstruction techniques. Med. Imag. Analysis 3(4), 339–359 (1999)
12. Seabra, J., Sanches, J.: Modeling log-compressed ultrasound images for radio frequency signal recovery. In: Engineering in Medicine and Biology Society (2008)
13. Seabra, J.C.R.: Medical ultrasound b-mode modeling, de-speckling and tissue characterization assessing the atherosclerotic disease. Ph.D. dissertation, Instituto Superior Técnico (May 2011)
14. Seabra, J., Xavier, J., Sanches, J.: Convex ultrasound image reconstruction with log-euclidean priors. In: IEEE Engineering in Medicine and Biology Society, EMBS 2008, pp. 435–438 (2008)
15. Solberg, O., Lindseth, F., Torp, H., Blake, R., Nagelhus Hernes, T.: Freehand 3D ultrasound reconstruction algorithms–a review. Ultrasound in Medicine & Biology 33(7), 991–1009 (2007)
16. Yin, W., Osher, S., Goldfarb, D., Darbon, J.: Bregman iterative algorithms for ℓ_1 minimization with applications to compressed sensing. SIAM Journal on Imaging Sciences 1(1), 143–168 (2008)
17. Yu, C., Zhang, C., Xie, L.: A multiplicative nakagami speckle reduction algorithm for ultrasound images. In: Multidim. Sys. and Sig. Proc., pp. 1–15 (2012)